A Modification of Path Integral Quantum Transition State Theory for Asymmetric and Metastable Potentials

Seogjoo Jang, Charles D. Schwieters,† and Gregory A. Voth*

Department of Chemistry and Henry Eyring Center for Theoretical Chemistry, University of Utah, 315 S. 1400 E. Rm Dock, Salt Lake City, Utah 84112-0850

Received: June 28, 1999; In Final Form: August 18, 1999

Path integral quantum transition state theory (PI-QTST) and its modified versions are studied for an asymmetric Eckart barrier and a metastable potential. For low temperatures, it is confirmed that the PI-QTST overestimates the reaction rate, as do other quantum activated rate theories. A simple correction method which modifies the product part of the potential such that it is bounded by the potential reactant well bottom energy is then implemented. The resulting tests for the asymmetric Eckart barrier and a cubic metastable potential demonstrate that this method gives a reliable estimate of the reaction rate for the model systems considered. For an understanding of the source of the error in the usual PI-QTST method and of the underlying mechanism of the correction, a detailed semiclassical analysis is then performed. This analysis demonstrates that the modified PI-QTST of Cao and Voth [Cao, J.; Voth, G. A. *J. Chem. Phys*. **1996**, *105*, 6856] becomes equivalent to the semiclassical bounce theory at low temperature only if a certain subset of classical paths is used. It is therefore concluded that the errors originate from the inappropriate mixing-in of paths associated with the product bound states in numerical path integral evaluations. These product paths are eliminated by the suggested correction method, thus rendering PI-QTST much more accurate for strongly asymmetric or metastable systems at low temperatures.

I. Introduction

From a molecular viewpoint, activated reaction events[1−9] are rare phenomena, and the probability that the system will visit the reactive zone, as determined by the free energy barrier, accounts for the dominant contribution to the reaction rate. Transition state theory (TST),[10] in this sense, amounts to the simplest approximation. It plays an important practical role in estimating the reaction rates in various systems and is indeed amenable to further improvement.[8,9] In generalizing TST to the quantum case,[1−7,11−13] however, one is confronted with some conceptual difficulties due to quantum dispersion and tunneling even in the simplest generic case of a single adiabatic barrier crossing.

Only in the two limiting cases of high and low temperature does the quantum description become simplified. In the former case, one can proceed in close analogy with classical picture by including a small amount of quantum dispersion and barrier top tunneling only.[14,15] In the zero temperature limit, within the path integral formalism,[16−19] one can identify with the reactant state those paths localized near the bottom of the reactant potential well. Barrier-crossing events are associated with paths which traverse from the reactant region to the product. Within the semiclassical approximation, the resulting rate can be expressed in terms of the properties of one (or more) periodic orbits on the inverted potential.[20−27]

The approaches used in the two limiting situations above are rather different, though the two results can be formally unified in a single mathematical expression.[24,25] In this context, Gillan's observation[28] and the ensuing work of Voth, Chandler, and Miller (VCM)[29] provided an important contribution. Gillan found that known reaction rate expressions for a symmetric double well potential coupled to a harmonic bath can be recast into classical-like forms employing the path centroid defined within the imaginary time path integral formalism.[16−19] Later, VCM carried out a more rigorous analysis, the outcomes of which are the path integral quantum TST (PI-QTST), a rigorous derivation of some of Gillan's results, and the idea of supplementing the approximate reaction rate with additional exact quantum dynamics calculations.

Subsequent tests and analyses[7,30−35] have shown that PI-QTST is very accurate in the high temperature limit and near the so called crossover temperature in which the dynamics begins to be dominated by tunneling. Below the crossover, it reproduces the dominant exponential term for symmetric or weakly asymmetric potentials, and it can be improved with a modification of the preexponential factor.[36,37] Recent work has focused on finding a more universal expression for this factor and also on the extension of the theory to nonadiabatic cases.[36,38−40] On the other hand, applications of the PI-QTST to strongly exothermic or metastable potentials at low temperature can be problematic. The reaction rate appears to be overestimated by orders of magnitude or, in fact, may not be defined in some cases.[33,41,42] The reason for this has been explained in a way analogous to classical multidimensional TST. In the general function space of cyclic paths, the centroid used in PI-QTST, the zeroth mode of the path, belongs to a specific class of dividing surfaces. For the case of asymmetric potentials, the optimal dividing surface seems to be rotated[42] in a direction different from any of the surfaces corresponding to a fixed centroid and the use of the centroid coordinate results in overestimation of the reaction rate. On the basis of this idea, Cao and Voth (CV)[36] and Mills et al.[42] independently developed

* Corresponding author.
† Present address: Computational Bioscience and Engineering Laboratory, NIH, Bethesta, MA 20892.

10.1021/jp992190+ CCC: $18.00
Published on Web 10/23/1999

schemes for identifying the optimum surface in the general function space of paths, one of which has been applied to some systems.[42] However, this approach may limit the application of the theory to small systems, so a more practical solution that does not abandon the practical merits of PI-QTST is still desirable.

Recently, two new approaches to a QTST have also appeared.[43−45] These start from an expression for the flux-side correlation function[46] and then invoke mathematically or physically motivated approximations. These new QTSTs produce results comparable to those of PI-QTST when tested for the symmetric Eckart barrier. For the case of asymmetric Eckart barrier, a detailed comparison has not been made, although the new theories have also been reported to perform unsatisfactorily.

The present paper was thus motivated by the incomplete understanding of the performance of PI-QTST for the cases of asymmetric and metastable potentials at low temperature. The first objective is to calculate the reaction rates based on PI-QTST for the asymmetric Eckart barrier and to compare these with published results for a collection of different QTSTs. The results presented show that, although the PI-QTST performs worse than the semiclassical bounce theory[20−27] below the crossover temperature, it is somewhat better than other simple QTSTs. However, these data again confirm that one should be cautious in applying the theory to asymmetric or metastable potentials at low temperature. The second objective is then to provide a simple, mathematically motivated, correction procedure to PI-QTST to render it again quantitatively accurate for such systems.

This paper is organized as follows: In section II, the PI-QTST and its improved versions using different preexponential factors are summarized and the results of their application to the asymmetric Eckart barrier are presented. In section III, a practical remedy is suggested for the strongly asymmetric barrier problem and then tested for the asymmetric Eckart barrier and for a cubic metastable potential. In section IV, a semiclassical analysis is made of the centroid density, which illuminates its relation with the semiclassical bounce theory and the sources of the errors involved in PI-QTST for strongly asymmetric system at low temperature. Section V provides concluding remarks.

II. Path Integral Transition State Theory Applied to An Asymmetric Eckart Barrier

A. Formal Expressions. The quantum partition function in the path integral formalism can be recast into the following classical-like form:[16,47,48]

$$Z \equiv Tr\{e^{-\beta\hat{H}}\} = \sqrt{\frac{m}{2\pi\hbar^2\beta}} \int dx_c \rho_c(x_c) \tag{1}$$

where β is the inverse temperature in units of the Boltzmann constant, m is the mass, and the "excess" centroid density beyond the free particle limit along the reaction coordinate is given by the path integration over all constrained cyclic paths such that

$$\rho_c(x_c) \equiv e^{-\beta V_c(x_c)} = \sqrt{\frac{2\pi\hbar^2\beta}{m}} \int \cdots \int D[x(\tau)]\, \delta(x_c - x_0) \exp\{-S[x(\tau)]/\hbar\} \tag{2}$$

with $x_0 = \int_0^{\beta\hbar} d\tau\, x(\tau)/(\beta\hbar)$. In eq 2, $D[x(\tau)]$ is the usual path measure[16−19] and $S[x(\tau)]$ is the Euclidean action functional,[16−19] defined as

$$S[x(\tau)] = \int_0^{\beta\hbar} d\tau \left\{\frac{m}{2}\dot{x}(\tau)^2 + V(x(\tau))\right\} \tag{3}$$

where $\dot{x}(\tau)$ is the derivative of $x(\tau)$ with respect to τ. A one-dimensional notation is used throughout for simplicity. Note that, as opposed to some of our earlier papers, the centroid potential of mean force $V_c(x_c)$ is defined here to be the excess centroid free energy over the free particle limit. The notation "$\rho_c(x_c)$" in this paper will also refer to the excess centroid density beyond the free particle limit, which is the important contribution to the rate constant.

The rate expression in PI-QTST,[7,29] expressed as $k_{PI-QTST}$ hereafter, has the following classical form:

$$k_{PI-QTST} = \frac{1}{2\pi\beta\hbar}\frac{e^{-\beta V_c(x_c^*)}}{Z_R} = \frac{(2\pi m\beta)^{-1/2}}{\int_{-\infty}^{x_c^*} dx_c e^{-\beta V_c(x_c)}} e^{-\beta V_c(x_c^*)} \tag{4}$$

where x_c^* corresponds to the barrier position of V_c and Z_R is the reactant state partition function. This rate expression is, in fact, the variational version of PI-QTST. At high temperature and for the inverted harmonic barrier, this expression has been shown to yield the exact high temperature result. Near or below the crossover temperature, however, eq 4 begins to underestimate the reaction rate for the symmetric Eckart barrier. Cao and Voth (CV)[36] have provided a unified expression for the preexponential factor which improves on this feature of the theory. They used Affleck's well-known correction factor[24] in a way consistent with the known high temperature result, and based on the assumption that the free energy saddle point in the general space of paths can be well represented by the centroid coordinate alone. The resulting expression is given by

$$k_{CV} = \min\left(\frac{\omega_b}{\omega_{c,b}}, \frac{2\pi}{\omega_{c,b}\beta\hbar}\right) k_{PI-QTST} \tag{5}$$

where ω_b is the frequency of the inverted harmonic function fitting the barrier top of $V(x)$ and $\omega_{c,b}$ is that fitting the barrier top of $V_c(x_c)$.

More recently, Ramirez[37] suggested a different uniform expression for the preexponential factor based on an empirical relation which seems to work well for the symmetric Eckart barrier. It is given by

$$k_R = \left(\frac{V_c(x_c^*)}{E_c(x_c^*)}\right)^{1/2} k_{PI-QTST} \tag{6}$$

where x_c^* is again understood as the position of the barrier top of V_c and $E_c(x_c)$ corresponds to an average energy for a fixed centroid minus $1/(2\beta)$, the Virial form[49,50] of which is given by

$$E_c(x_c) = \left\langle \frac{1}{2}(x(\tau) - x_c)V'(x(\tau)) + V(x(\tau)) \right\rangle_c \tag{7}$$

where $\langle\cdots\rangle_c$ means average over the centroid constrained path integral of eq 2.

B. Results. The reaction rates were calculated for the following asymmetric Eckart barrier:

$$V(x) = \frac{A}{1 + e^{-ax}} + \frac{B}{4\cosh^2(ax/2)} \tag{8}$$

with $V(-\infty) = 0$, $V(\infty) = A = -18/\pi$, $B = 54/\pi$, and $a =$

$\sqrt{3\pi}/4$. Natural units have been chosen such that $\hbar = \omega_b = m = 1$. These choices of parameters and units result in a classical barrier height of $V^* = 6/\pi$ and a classical barrier location of $q^* = -\ln 2/a$. The quantity to be compared is Γ, the ratio of the quantum rate to the classical rate. Thus, calculation of the reaction rates requires the determination of $V_c(x_c)$ defined by eq 2, and the average centroid energy function given by eq 7 if Ramirez's expression for the rate is used. These calculations can be performed using any path integral simulation method, along with the imposition of the centroid constraint.

The method of staging path integral molecular dynamics (SPIMD) was chosen in the present work.[51] The number of quasiparticles, $P = 25\beta$, gave converged thermodynamic data for all the values of β tested. The number of primary quasiparticles used was 10 for all temperatures, and each intervening segment consisting of $P/10-1$ quasiparticles was transformed into staging coordinate. To ensure canonical sampling, a Nosé−Hoover chain[52] of length 4 was attached to each transformed degree of freedom. The use of this thermostat in the presence of the centroid constraint was made possible using modified NHC equations of motion,[53] which account for the constrained degree of freedom correctly, and by employing one of the corresponding simple reversible velocity Verlet type algorithms, VV-3.[53] The mass of the primary quasiparticle was chosen to be $P/10$, the mass of the kth ($k = 1, \cdots, P/10-1$) staging transformed coordinate was chosen to be $P^2(k+1)/(100k)$, and the Nosé mass was set to $0.012P$. A time step of $6.32 \times 10^{-4}P$ was used in the simulation.

The centroid mean force was calculated using

$$F_c(x_c) = \langle F(x(\tau))\rangle_c = -\frac{d}{dx_c} V_c(x_c) \qquad (9)$$

while eq 7 was used for the average centroid energy. These quantities were calculated at successive centroid positions from -12 to 12, in increments of 0.2. At each given value of x_c, the system was equilibrated for 10^5 steps and then sampled for 2×10^6 steps. The centroid potential of mean force $V_c(x_c)$ was then calculated by the integration of the centroid mean force, using cubic interpolation and quadratic extrapolation where necessary.

Figure 1 shows the calculated centroid potentials of mean force and the average centroid energies for six different values of β. As β increases (temperature decreases), the maximum value of V_c decreases and its position shifts toward the reactant side. Table 1 presents the ratio Γ for various versions of PI-QTST, identified by subscript. In calculating the reaction rate, significant figures were kept to three and all the calculated V_c's were rounded off up to the second decimal point. The results of other QTSTs are also shown, along with the results due to the semiclassical bounce method calculated using the standard procedure.[20,24,54] In this table, Γ_{HA} represents the QTST2 results by Hansen and Andersen,[44] Γ_{PL} represents the QTST results by Pollak and Liao,[45] and Γ_{SPL} is the best perturbation expansion results taken from Table 3 of the paper by Shao et al.[55] The table shows that PI-QTST gives results comparable to Γ_{SPL}, a complicated variational perturbation theory, thus implying that the PI-QTST includes a substantial part of the nontrivial anharmonic contributions. The expression of CV improves these results further, remaining quite close to the exact ones. On the other hand, the expression of Ramirez seems to worsen the estimation of the PI-QTST, which indicates that his present empirical relation may not have much generality beyond the symmetric limit.

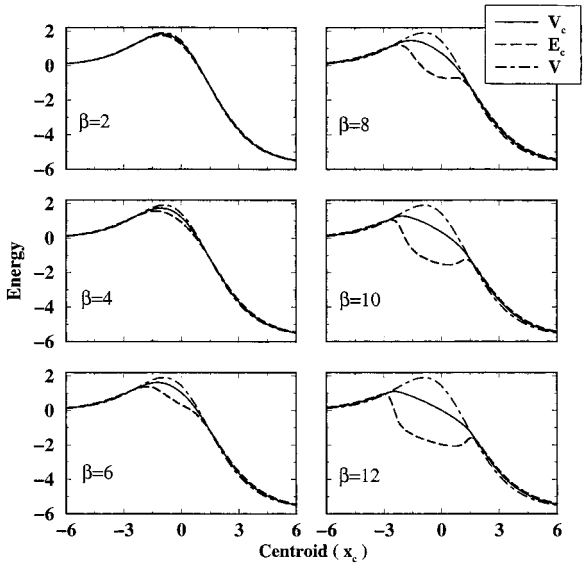

Figure 1. Centroid potential of mean force (V_c) and average energy function (E_c) as a function of the centroid x_c compared with the classical potential, for the asymmetric Eckart barrier given by eq 8, at six different values of β.

TABLE 1: Ratio of QTSTs to the Classical TST, Denoted as Γ, for the Asymmetric Eckart Barrier of eq 8

β	$\Gamma_{PI-QTST}$[a]	Γ_{CV}[b]	Γ_R[c]	Γ_{HA}[d]	Γ_{PL}[e]	Γ_{SLP}[f]	Γ_{sc}[g]	Γ_{ex}[h]
2	1.17	1.23	1.20	1.2	1.2	1.2		1.2
4	1.97	2.16	2.09	2.0	2.0	2.0		2.0
6	5.69	6.35	6.58	5.2	5.6	5.4		5.3
8	36.6	30.6	50.9	38	44	31	28.1	26
10	544	335	925	1100	1100	655	233	250
12	16600	7620	65000	87000	28000	13100	3710	4100

[a] Path integral quantum transition state theory (PI-QTST). [b] Cao and Voth modification of PI-QTST. [c] Ramirez modification of PI-QTST. [d] QTST2 by Hansen and Andersen. [e] QTST by Pollak and Liao. [f] The best perturbation expansion result calculated by Shao, Liao, and Pollak. [g] Semiclassical bounce theory. [h] Exact result.

It is seen that PI-QTST overestimates the rate at lower temperature, while the CV modification is most successful. However, it is still in error by almost a factor of two at $\beta = 12$. These results are in contrast to those of the semiclassical bounce theory which somewhat underestimates the exact rate, but achieves agreement to within a few percent. This situation seems to contradict the analysis by VCM,[29] which showed that the semiclassical limit of PI-QTST can be made equivalent to the bounce theory by a modification of the preexponential factor only. Indeed PI-QTST performs quite well for the case of the symmetric Eckart barrier, but not as well for the asymmetric case.

III. Simple Correction Method

The data calculated in section II are consistent with the previous findings regarding the performance of PI-QTSTs for asymmetric or metastable potentials.[41,42] Makarov and Topaler[41] provided an insightful analysis and suggested a simple correction method where the underlying potential energy $V(x)$ in the calculation is modified to be $\max\{V(x), V_{cut}\}$ with V_{cut} chosen to be an arbitrary number smaller than the potential reactant well bottom energy. They tested this method for a cubic metastable potential.[41] Above the cross-over temperature, the results were in close agreement with the exact one irrespective of the choice of V_{cut}. However, below the crossover, they found the results become sensitive to the value of V_{cut} and are not as reliable as those calculated by the semiclassical bounce theory.[56]

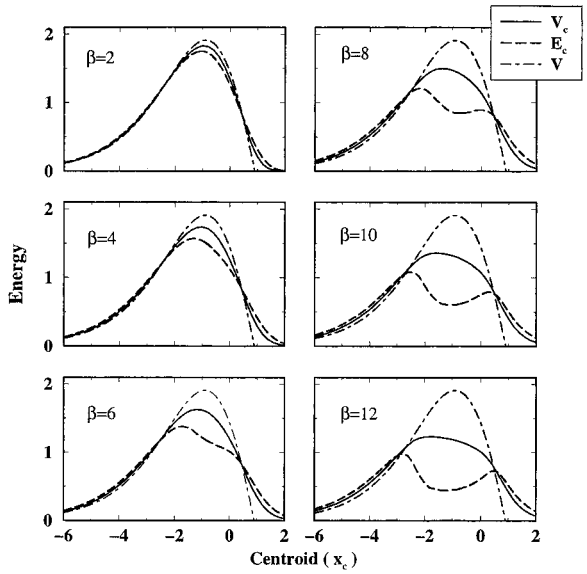

Figure 2. Centroid potential of mean force (V_c) and average energy function (E_c) as a function of the centroid x_c compared with the classical potential, for the asymmetric Eckart barrier given by eq 8 modified in the way of eq 10, at six different values of β.

TABLE 2: Ratio of PI-QTSTs to the Classical TST for the Asymmetric Eckart Barrier of Equation 8 Modified by the Way of Equation 10[a]

β	$\Gamma_{PI-QTST}$	Γ_{CV}	Γ_R	Γ_{sc}	Γ_{ex}
2	1.17	1.23	1.20		1.2
4	1.97	2.19	2.09		2.0
6	5.36	6.65	6.07		5.3
8	26.5	30.7	33.1	28.1	26
10	244	287	346	233	250
12	3490	4140	5560	3710	4100

[a] The symbols are as described in Table 1. The semiclassical bounce theory and the exact results for the original potential are provided for reference.

In the present paper, we suggest and more clearly justify the use of a similar correction method, but with the value of V_{cut} always fixed to be that of the potential reactant well bottom energy. That is, given a potential, the reaction rates are calculated by applying PI-QTST and its modifications to the following potential:

$$V(x) = \begin{cases} V(x), & V(x) \geq V_r \\ V_r, & V(x) < V_r \end{cases} \qquad (10)$$

with V_r being the reactant well bottom energy.

First, the asymmetric Eckart barrier considered in the previous section was tested, where $V_r = 0$. The potential used in the simulation was the original potential for $x \leq 0.9$ and a Gaussian tail joined at $x = 0.9$ such that the potential and the first derivative change continuously. Since the value of the potential at the joining point is very small (about 0.006) and the Gaussian tail decays to zero rapidly, this method of modification is practically the same as the one suggested by eq 10. Numerical calculation of the centroid potential of mean force V_c was then performed as described in section II.B. Figure 2 shows the potentials for six different values of β. Table 2 shows the calculated values of Γ, using the three PI-QTST based approaches with the modified potential. The semiclassical and exact results given in Table 1 are shown again for reference. As can be seen in Table 2, the modified PI-QTST results all show much better agreement with the exact ones.

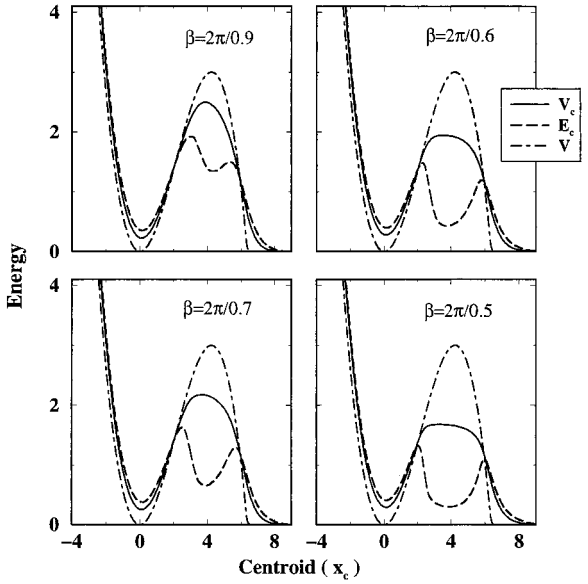

Figure 3. Centroid potential of mean force (V_c) and average energy function (E_c) as a function of the centroid x_c compared with the classical potential, for the metastable cubic potential of eq 11 modified in the way of eq 10, at four different values of β below the crossover temperature.

In this case, the PI-QTST underestimates the reaction rate, a trend similar to the case of the symmetric Eckart barrier.[29,36,37] The CV reaction rate expression corrects the PI-QTST results in the right direction and provides the best estimates for the reaction rates below the crossover temperature. The rates calculated by Ramirez's expression also differ from the PI-QTST results in the proper direction, but below the crossover temperature, it results in a much larger overestimation of the rate than the CV result.

As an additional test case, the same approach was implemented for a cubic metastable potential that was previously treated by Makarov and Topaler.[41] The explicit form of the model potential is given by

$$V(x) = \frac{1}{2}x^2 - \frac{1}{9\sqrt{2}}x^3 \qquad (11)$$

with the same natural units as before. For this potential, $x_b = 3\sqrt{2}$ and $V_b = 3$. Since $\omega_b = 1$, the crossover value of β is equal to 2π. For the present case also, $V_r = 0$. The potential was modified in a similar way as before by joining the original potential with a Gaussian tail at $x = 6.3$. Four different values of β below the cross-over temperature were considered. For a given value of β, the number of path integral quasiparticles was chosen to be $180\beta/(2\pi)$, and the number of primary quasiparticles was set to 10. The staging transformation was made for each intervening segment as before. The centroid mean force was calculated in the same way as before by varying the centroid with the interval of 0.2 in the range from -3 to 12. Figure 3 shows the centroid potential of mean force, and Table 3 compares the calculated reaction rates with the exact ones.[56] The rates based on the semiclassical bounce theory have again been calculated according to the standard method.[20,24,54] For this case also, the CV theory gives quite accurate results and becomes comparable to the semiclassical approximations in the low temperature limit, except for the case of $\beta = 2\pi/0.5$, where the deviation seems simply originate from the breakdown of the stationary phase integration approximation in the centroid variable space. As can be seen from Figure 3, the centroid

TABLE 3: Reaction Rate Calculated by PI-QTSTs Modified in the Way of Equation 10 for the Cubic Metastable Potential of Equation 11[a]

β	$k_{PI-QTST}$	k_{CV}	k_{sc}	k_{ex}
$2\pi/0.9$	1.90	2.16	2.45	1.92 ($\times 10^{-8}$)
$2\pi/0.7$	4.63	6.47	7.26	6.77 ($\times 10^{-9}$)
$2\pi/0.6$	3.91	6.24	6.26	5.83 ($\times 10^{-9}$)
$2\pi/0.5$	3.97	7.61	6.02	5.60 ($\times 10^{-9}$)

[a] The reaction rates are denoted as k with the subscripts having the same meaning as in Table 1. The semiclassical bounce theory and the exact results are for the original potential. For the units, refer to the main text.

potential of mean force cannot be well approximated by a quadratic function down to the energy comparable to k_BT. Therefore, the result could be improved by using an effective curvature rather than the one at the barrier top.

The results of the two test cases show that the CV theory applied to the modified potential of eq 10 predicts reaction rates comparable to those based on the semiclassical bounce theory below the cross-over temperature. This implies that when the choice of $V_{cut} = V_r$ is made, the centroid coordinate recovers its role as the proper reaction coordinate and the action for this modified potential at the local maximum in the centroid variable space is very close to the action for the original potential at the saddle point in the general space of paths. In the following section, a detailed semiclassical analysis of the centroid density is provided, which illuminates the source of the error involved in the original applications of PI-QTST and CV theory to strongly asymmetric and metastable potentials, as well as the mechanism of the correction made by the simple remedy suggested here.

IV. Semiclassical Centroid Density

A. General Expressions. In the present section, a semiclassical expression for the excess centroid density is provided. For this purpose, eq 2 is rewritten as

$$\rho_c(x_c) = \sqrt{\frac{2\pi\hbar^2\beta}{m}} \int_{-\infty}^{\infty} \frac{d\zeta}{2\pi} \int_{-\infty}^{\infty} dx \int \cdots \int_x D'[x(\tau)] \times \exp\{-S[x(\tau)]/\hbar + i\zeta(x_0 - x_c)\} \quad (12)$$

where the delta function in the integrand of eq 2 has been replaced with its Fourier integral expression. The path integration is over those paths with $x(0) = x(\beta\hbar) = x$ as indicated by the subscript of the path integral, and the prime in the path measure indicates that the integration over x has been singled out. In the semiclassical limit, the dominant contribution of this integral comes from paths close to the classical paths on the inverted potential. These paths can be decomposed into

$$x(\tau) = x_{cl}(\tau) + \delta x(\tau) \quad (13)$$

where $x_{cl}(\tau)$ is a classical path on the inverted potential satisfying the boundary condition $x_{cl}(0) = x_{cl}(\beta\hbar) = x$, and $\delta x(\tau)$ is an arbitrary fluctuation away from the classical path with the restriction $\delta x(0) = \delta x(\beta\hbar) = 0$. Including up to the second order variation of the action with respect to $\delta x(\tau)$, the semiclassical approximation for the centroid density of eq 12 is given by

$$\rho_c^{sc}(x_c) = \int dx \sum_{Cl(x)} e^{-S[Cl(x)]/\hbar} I[x_c, Cl(x)] \quad (14)$$

where $Cl(x)$ is a classical trajectory starting at x and ending at the same point after an interval $\tau = \beta\hbar$, and the summation implies that there can be more than one such trajectory. The quantity $I[x_c, Cl(x)]$ is a centroid-constrained quadratic path integral, which depends on x_c, x, and on the specific classical orbit chosen. This quantity is defined as

$$I[x_c, Cl(x)] = \sqrt{\frac{\hbar^2\beta}{2\pi m}} \int_{-\infty}^{\infty} d\zeta \exp\{i\zeta(x_{cl,0} - x_c)\} \times \int \cdots \int_0 D'[\delta x(\tau)] \exp\left\{-\frac{m}{2\hbar}\int_0^{\beta\hbar} d\tau \int_0^{\beta\hbar} d\tau' \, \delta x(\tau) \times L(\tau, \tau') \, \delta x(\tau') + \frac{i\zeta}{\beta\hbar} \int_0^{\beta\hbar} d\tau \, \delta x(\tau)\right\} \quad (15)$$

with $x_{cl,0} = \int_0^{\beta\hbar} x_{cl}(\tau)/(\beta\hbar)$ and

$$L(\tau, \tau') = \left\{-\frac{\partial^2}{\partial\tau^2} + \frac{1}{m} V''(x_{cl}(\tau))\right\} \delta(\tau - \tau') \quad (16)$$

Note that these latter objects also implicitly depend on the value of x and on the specific classical orbit chosen. The subscript of 0 in the path integral of eq 15 indicates that $\delta x(\tau)$ starts and ends at zero. For the differential operator of eq 16, the zero eigenvalue Green function[19,57,58] can be defined by the following relation:

$$\int_0^{\beta\hbar} d\tau' \, L(\tau, \tau') \, G(\tau', \tau'') = \int_0^{\beta\hbar} d\tau' \, G(\tau, \tau') \, L(\tau', \tau'') = \delta(\tau - \tau'') \quad (17)$$

which satisfies the same boundary condition as $\delta x(\tau)$ stated above. It will be shown later that the explicit expression for the semiclassical centroid density involves this Green function. For the time being, it is assumed that the operator of eq 16 does not have a zero eigenvalue so that the Green function defined by eq 17 is not singular. Later, it will be shown that the case with zero eigenvalue can be included as a limiting case in performing the final integration.

Equation 15 can be transformed into an expression involving a solution of the differential equation of eq 16 and an integration over the Green function defined by eq 17. The detailed method of evaluation and the final expression depend on whether or not the differential operator of eq 16 has a negative eigenvalue. Appendix A starts with the discretized approximation for eq 15 and then provides a general expression which allows explicit Gaussian integrations. For the case where all the eigenvalues are positive, the Gaussian integrations over all the fluctuation modes can be performed without any ambiguity, and this is described in Appendix B. The case where there is a single negative eigenvalue and no zero eigenvalue is treated in Appendix C. Here greater care must be taken with the order of integration, and the existence of the result is seen to depend on the shape of the potential.

The expression in eq 14 shows that a given semiclassical centroid density, whether it is convergent or divergent, can be formally decomposed into disjoint components, which we characterize by the specific classical orbits. All of the nonstationary classical trajectories must have at least one turning point because of the boundary condition $x_{cl}(0) = x_{cl}(\beta\hbar)$. Since a given classical trajectory spends a substantial part of its time near the turning point(s), the characteristics of each component of the semiclassical centroid density given by eq 14 can be related to the nature of the turning points. Thus it is reasonable to decompose the semiclassical centroid density into components

associated with the location of the turning points of their underlying classical trajectories, as follows:

$$\rho_c^{sc}(x_c) = \rho_{c,r}^{sc}(x_c) + \rho_{c,b}^{sc}(x_c) + \rho_{c,p}^{sc}(x_c) \tag{18}$$

where the subscripts *r*, *b*, and *p* respectively represent the reactant, the barrier, and the product parts of the centroid density. For more quantitative statement, we temporarily introduce dividing surfaces: d_{rb}, which lies between the reactant bottom and the barrier top, and d_{bp}, which lies between the barrier top and the product bottom. In most situations where the reaction rate can be defined, although somewhat arbitrary, these dividing surfaces can always be found such that, in the classical limit, the reactant region of the configuration space corresponds to the lefthand side of d_{rb} and the product region of the configuration space corresponds to the righthand side of d_{bp}. Within the semiclassical approximation, the turning points of the underlying classical trajectories can play such roles. That is, the reactant centroid density, $\rho_{c,r}^{sc}(x_c)$, is the centroid density around the classical trajectories with all of their turning points at the left hand side of d_{rb} ; and vice-versa for the product centroid density. The barrier centroid density is the centroid density around those classical trajectories with the turning points in between d_{rb} and d_{bp}, and around those classical trajectories with turning points on both the lefthand side of d_{rb} and the righthand side of d_{bp}. In the high temperature limit, only the former contributes to the barrier centroid density, and the latter appears only below some temperature in most cases and becomes more dominant as the temperature goes down. The details of the decomposition depend on the topology of the potential and the temperature. In the following, the simple generic case is considered where the regions near the reactant bottom and the barrier top can be well approximated by quadratic functions and where the potential changes in a smooth and continuous fashion between these regions.

B. Reactant Centroid Density. Due to the generic shape of the potential assumed in the analysis, the reactant centroid density consists of those classical trajectories which have only one turning point on the reactant side hill of the inverted potential. Such trajectories, denoted as Cl(*x*; *r*), start at *x*, approach (from either side) the top of the reactant side hill of the inverted potential without crossing it, and then after a time $\beta\hbar$, return to their original position *x*, with momentum at $\tau = \beta\hbar$ equal in magnitude and opposite in sign to that at $\tau = 0$. Note that there is only one such trajectory for given *x* and $\beta\hbar$. The stationary trajectory sitting at the top of the hill can be included as a limiting situation of these trajectories. The general expression is given by

$$\rho_{c,r}^{sc}(x_c) = \int_r dx\, e^{-S[Cl(x;r)]/\hbar}\, I[x_c, Cl(x; r)] \tag{19}$$

where $I[x_c, Cl(x; r)]$ is the centroid constrained quadratic path integration defined by eq 15 around the classical trajectory of Cl(*x*; *r*). The subscript of *r* denotes that the integration is performed only for *x* satisfying the condition of $x_{cl}(\beta\hbar/2) < d_{rb}$. At high enough temperature, $\beta\hbar$ is small and the starting point *x* should be close to the turning point. Thus, the dominant contribution to eq 19 is from the reactant bottom region of the original potential, which can be approximated by the following harmonic potential:

$$V(x) \approx V_r + \frac{m\omega_r^2}{2}(x - x_r)^2 \tag{20}$$

Then, the classical trajectory on the inverted potential satisfying the boundary condition is given by

$$x_{cl}(\tau) = x_r + (x - x_r)\frac{\cosh(\omega_r(\beta\hbar/2 - \tau))}{\cosh(\omega_r \beta\hbar/2)} \tag{21}$$

The center of this trajectory, the time average, is given by

$$x_{cl,0} = x_r + (x - x_r)\frac{2}{\omega_r\beta\hbar}\tanh(\omega_r\beta\hbar/2) \tag{22}$$

and the action along the given trajectory is given by

$$S_{cl} = \beta\hbar V_r + m\omega_r(x - x_r)^2\tanh(\omega_r\beta\hbar/2) \tag{23}$$

For the given trajectory, the second derivative of the potential is constant and the differential operator defined by eq 16 simplifies to

$$L(\tau, \tau') = \left(-\frac{\partial^2}{\partial\tau^2} + \omega_r^2\right)\delta(\tau - \tau') \tag{24}$$

which is independent of *x*. This operator does not have any negative or zero eigenvalues and the centroid-constrained path integral of $I[x_c, Cl(x; r)]$ in eq 19 can be calculated as described in Appendix B. For the present case, the explicit expressions for eqs B3 and B5 can be shown to be

$$f(\beta\hbar) = \frac{1}{\omega_r}\sinh(\omega_r\beta\hbar) \tag{25}$$

$$\gamma = \left(\frac{b\hbar}{\omega_r}\right)^2\left(1 - \frac{2}{\omega_r\beta\hbar}\tanh\left(\frac{\omega_r\beta\hbar}{2}\right)\right) \tag{26}$$

Inserting eqs 22, 25, and 26 into eq B6, and then using the resulting expression in eq 19 along with eq 23 one can obtain an expression for the reactant centroid density which involves Gaussian integration over *x*. Performing this integration, the following high temperature expression is obtained:

$$\rho_{c,r}^{sc}(x_c) \approx \frac{(\omega_r\beta\hbar/2)}{\sinh(\omega_r\beta\hbar/2)}\exp\left\{-\beta V_r - \frac{\beta m\omega_r^2}{2}(x_c - x_r)^2\right\} \tag{27}$$

As the temperature is reduced, the imaginary time $\beta\hbar$ becomes larger and the important classical trajectories sample a larger region of the potential, away from the reactant minimum. Eventually, the harmonic approximation for the potential will break down. However, as long as the curvature of the original potential increases as the trajectories approach the turning point, all the eigenvalues of the differential operator of eq 16 remain positive and the semiclassical centroid density can be evaluated in the same manner of Appendix B. Although it is not in general possible to find the explicit expressions for the eigenvalue spectrum and the Green function, one can usually make an effective harmonic approximation and the final expression can be brought into the form of eq 27 with the frequency ω_r replaced with the x_c dependent effective frequency $\Omega_r(x_c)$. Note that the value of $\rho_{c,r}^{sc}(x_c)$ decreases in a Gaussian fashion as the centroid x_c is moved away from the reactant minimum x_r toward the barrier top. This feature will be revisited later in the analysis of the simple correction scheme.

C. Barrier Centroid Density. The barrier centroid density consists of those classical trajectories which connect the reactant

and the product sides of the potential. At high enough temperature (small $\beta\hbar$), the only possible trajectories of this kind are those concentrated near the barrier region. On the other hand, at temperatures low enough that $\beta\hbar$ is larger than the period of the small harmonic oscillation near the barrier region, periodic orbits with much lower action exist and the paths near these orbits represent the dominant contribution to barrier crossing.

1. High Temperature Limit. In this case there is no periodic orbit crossing the barrier top of the original potential, and the only possible trajectories are those which start near the local minimum of the inverted potential, climb up toward either the reactant or the product side slightly, and then return to their original position. The constant trajectory sitting at the local minimum of the inverted potential is included as a limiting case of these trajectories. The expression for the barrier region centroid density, therefore, can be written as

$$\rho_{c,b}^{sc}(x_c) = \int_b dx\, e^{-S[Cl(x)]/\hbar}\, I[x_c, Cl(x; b)] \tag{28}$$

where the subscript b implies that the integration is done only for x satisfying $d_{rb} < x_{cl}(\beta\hbar/2) < d_{bp}$ and $I[x_c, Cl(x; b)]$ is the centroid constrained quadratic path integration defined by eq 15 around the barrier region classical trajectory of $Cl(x; b)$. Again, it is assumed that the potential in this region can be well approximated by the inverted parabolic form

$$V(x) \approx V_b - \frac{m\omega_b^2}{2}(x - x_b)^2 \tag{29}$$

Then, for a given x, there exists a unique classical trajectory on the inverted potential satisfying the boundary condition as follows:

$$x_{cl}(\tau) = x_b + (x - x_b)\frac{\cos(\omega_b(\tau - \beta\hbar/2))}{\cos(\omega_b\beta\hbar/2)} \tag{30}$$

This expression becomes singular when $\beta\hbar = \pi/\omega_b$. For the moment, it is assumed that $\beta\hbar < \pi/\omega_b$. The time average of this trajectory, its centroid, is given by

$$x_{cl,0} = x_b + (x - x_b)\frac{\tan(\omega_b\beta\hbar/2)}{(\omega_b\beta\hbar/2)} \tag{31}$$

and the action along the trajectory is given by

$$S_{cl} = \beta\hbar V_b - m\omega_b(x - x_b)^2 \tan(\omega_b\beta\hbar/2) \tag{32}$$

For the trajectory of eq 30, the differential operator defined by eq 16 simplifies to

$$L(\tau, \tau') = \left(-\frac{\partial^2}{\partial\tau^2} - \omega_b^2\right)\delta(\tau - \tau') \tag{33}$$

The eigenvalues of this operator are all positive under the limitation of $\beta\hbar < \pi/\omega_b$ as stated above, and the centroid constrained path integration $I[x_c, Cl(x)]$ in eq 28, can be calculated in the manner of Appendix B. The explicit expressions for eqs B3 and B5 can be calculated to be

$$f(\beta\hbar) = \frac{1}{\omega_b}\sin(\omega_b\beta\hbar) \tag{34}$$

$$\gamma = \left(\frac{\beta\hbar}{\omega_b}\right)^2\left(\frac{2}{\omega_b\beta\hbar}\tan\left(\frac{\omega_b\beta\hbar}{2}\right) - 1\right) \tag{35}$$

Inserting eqs 31, 34, and 35 into eq B6, and then using the resulting expression in eq 28 along with eq 32, one can obtain the following expression for the barrier centroid density:

$$\rho_{c,b}^{sc}(x_c) \approx \sqrt{\frac{\omega_b\beta\hbar}{\sin(\omega_b\beta\hbar)}}\sqrt{\frac{m\beta^3\hbar^2}{2\pi\gamma}}\, e^{-\beta V_b + \beta m\omega_b^2(x_c - x_b)^2/2}\int_{-\infty}^{\infty} dx \times \exp\left\{-\frac{m\beta^2\hbar}{\omega_b\gamma}\tan(\omega_b\beta\hbar/2)\,(x - x_c)^2\right\} \tag{36}$$

Since γ is positive, the Gaussian integration over x is defined and the resulting centroid density can be written as

$$\rho_{c,b}^{sc}(x_c) \approx \frac{(\omega_b\beta\hbar/2)}{\sin(\omega_b\beta\hbar/2)}\exp\left\{-\beta V_b + \frac{\beta m\omega_b^2}{2}(x_c - x_b)^2\right\} \tag{37}$$

This is equal to the exact centroid density for the inverted harmonic oscillator with frequency ω_b.

As has been stated, the derivation of eq 37 is valid only when $\beta\hbar < \pi/\omega_b$. For the case where $\pi/\omega_b \le \beta\hbar < 2\pi/\omega_b$, two difficulties are encountered in its derivation even though the final expression of eq 37 can still be used. First, the classical equation of motion, eq 30 becomes singular at $\beta\hbar = \pi/\omega_b$. The reason is that, at this temperature, the classical trajectory starting at x always ends up at $2x_b - x$ after half the period time, within the harmonic approximation, and the only solutions satisfying the given boundary condition are those trajectories starting at $x = x_b$. For values of $\beta\hbar$ slightly larger than that corresponding to the half-period, the classical solution of eq 30 can be used again. Second, when $\pi/\omega_b < \beta\hbar < 2\pi/\omega_b$, there appears a negative eigenvalue, and one cannot perform the path integral as described in Appendix B; nor can the approach of Appendix C be used because α_1 of the unstable mode appearing in eq C1 vanishes, making the resulting centroid density undefined. In fact, there exists an anharmonic contribution which was not considered above but resolves the difficulties stated here. That is, a small participation of the anharmonicity removes the singularity at $\beta\hbar = \pi/\omega_b$ and allows α_1 of the unstable mode to survive. Therefore, the centroid density changes continuously at the singularity and the method of Appendix C can be used in the range of $\pi/\omega_b < \beta\hbar < 2\pi/\omega_b$ as long as other criteria are satisfied. Thus, while anharmonic contributions from a realistic potential become crucial to the definition of the centroid density in this parameter regime, the qualitative behavior of the solution seems to remain the same as that for higher temperatures. That is, the final expression for the centroid density is expected to be well approximated by the form given by eq 37, with the barrier frequency ω_b replaced with an x_c-dependent effective harmonic barrier frequency, $\Omega_b(x_c)$.[29]

2. Low Temperature Limit. Below the temperature defined by $\beta\hbar = 2\pi/\omega_b$, there appear one or more periodic orbit(s) which bridge the reactant and the product regions. A feature of these trajectories is that the action along the trajectory does not depend on the choice of the initial position. The dominant contribution comes from the periodic orbit with period $\beta\hbar$, and the semiclassical barrier centroid density is approximated to be

$$\rho_{c,b}^{sc}(x_c) \approx e^{-S_{po}/\hbar}\int_{po} dx\, I[x_c, Cl(x; po)] \tag{38}$$

where S_{po} is the action along the periodic orbit and $I[x_c, Cl(x; po)]$ is the centroid-constrained path integral defined by eq 15

along the periodic orbit. The integration subscript of po implies that integration over x are performed along the points in the given periodic orbit.

For the special case where x corresponds to a turning point, $\dot{x}_{po}(\tau)$, becomes the zero eigenvalue solution of the differential operator of eq 16 satisfying the given boundary condition of $\dot{x}_{po}(0) = \dot{x}_{po}(\beta\hbar) = 0$. Otherwise, $\dot{x}_{po}(\tau)$ does not vanish at the boundary and the true solution should be obtained through a perturbative correction. This correction forces the solution to vanish at the boundary and the resulting eigenvalue becomes slightly larger than zero in a way analogous to a free particle confined to a one dimensional box with an infinite wall.[19] On the other hand, this (almost) zero eigenvalue mode has one node, which implies that there should be a solution without any node which has a negative eigenvalue.

Given the qualitative feature above, the calculation of $I[x_c, \mathrm{Cl}(x; \mathrm{po})]$ can be made as described in Appendix C, except for the case where $\dot{x}_{po}(0) = \dot{x}_{po}(\beta\hbar) = 0$, which will be included as a limiting case later. Since $\dot{x}_{po}(0) = \dot{x}_{po}(b\hbar)$ and the period of the orbit is independent of the initial point x, eq C8 simplifies to[59]

$$f(\beta\hbar) = m\dot{x}_{po}(0)^2 \frac{\mathrm{d}(\beta\hbar)}{\mathrm{d}E} \tag{39}$$

where E is the negative of the energy of the periodic orbit on the inverted potential. In the present case, the existence of a negative eigenvalue is equivalent to the condition that $\mathrm{d}(\beta\hbar)/\mathrm{d}E < 0$. Inserting the expression of eq 39 into eq C6 and then using the resulting expression in eq 37, the barrier centroid density can be written as

$$\rho^{sc}_{c,b}(x_c) \approx \mathrm{e}^{-S_{po}/\hbar} \int \mathrm{d}\dot{x}_{po}(0) \frac{1}{|\dot{x}_{po}(0)|} \sqrt{\frac{\mathrm{d}E}{\mathrm{d}(\beta\hbar)} \frac{\beta^2\hbar}{2\pi\gamma}} \times \exp\left\{-\frac{m\beta(x_{po,0} - x_c)^2}{2\gamma}\right\} \tag{40}$$

with γ defined by eq C14 having the following form for the present case:

$$\gamma = \frac{m}{\beta\hbar} \frac{\mathrm{d}(\beta\hbar)}{\mathrm{d}E} \left\{\frac{\partial}{\partial(\beta\hbar)} \int_0^{\beta\hbar} \mathrm{d}\tau\, x_{po}(\tau; \beta\hbar)^2 - \left(\frac{\partial}{\partial(\beta\hbar)} \int_0^{\beta\hbar} \mathrm{d}\tau\, x_{po}(\tau; \beta\hbar)\right)^2\right\} \tag{41}$$

Since $\mathrm{d}(\beta\hbar)/\mathrm{d}E$ is negative, the condition of $\gamma < 0$, a necessary condition for the existence of the semiclassical barrier centroid density, is equivalent to the condition that the quantity within the curly bracket of eq 41 is positive, which seems to be satisfied in most cases.[29]

Equation 40 can be simplified further.[59] The differential of $\mathrm{d}x_{po}(0)/|\dot{x}_{po}(0)|$ can be replaced with $\mathrm{d}\tau$, thereby also including the limiting case of $\dot{x}_{po}(0) = 0$. The rest of the integrand is independent of τ. Therefore, after the integration over τ, the final expression for the barrier centroid density is given by

$$\rho^{sc}_{c,b}(x_c) \approx \beta\hbar \mathrm{e}^{-S_{po}/\hbar} \sqrt{\frac{\mathrm{d}E}{\mathrm{d}(\beta\hbar)} \frac{\beta^2\hbar}{2\pi\gamma}} \exp\left\{-\frac{m\beta(x_{po,0} - x_c)^2}{2\gamma}\right\} \tag{42}$$

where both $\mathrm{d}E/\mathrm{d}(\beta\hbar)$ and γ are negative.

D. Product Centroid Density. The product centroid density consists of the classical trajectories which have all the turning points on the product side hill of the inverted potential. Representing these trajectories as $\mathrm{Cl}(x; \mathrm{p})$, the centroid density can be expressed as

$$\rho^{sc}_{c,p}(x_c) = \int_p \mathrm{d}x \sum_{\mathrm{Cl}(x;\mathrm{p})} \mathrm{e}^{-S[\mathrm{Cl}(x;\mathrm{p})]/\hbar} I[x_c, \mathrm{Cl}(x; \mathrm{p})] \tag{43}$$

where all the symbols have meanings analogous to those in the reactant centroid density of eq 19 and a general situation is considered such that the product region can have an arbitrary shape allowing multiple classical trajectories and the product side of the original potential can be either bounded or unbounded. While a formal definition of this product centroid density has been possible, there is no guarantee that it can always have a convergent value for the case of an unbounded product state. If the potential decrease is steep, either the path integration or the final integration over x in eq 43 can be divergent. On the other hand, if the product side of the original potential is bounded or it decreases less steeply than a quadratic function, it always has a convergent value.

For the purpose of the analysis to be made in the following section, an approximate explicit form for the product centroid density (when it converges) is useful. Again an effective harmonic expression is used for this purpose. In analogy with the reactant centroid expression of eq 27, the final result is given by

$$\rho^{sc}_{c,p}(x_c) \approx \frac{(\Omega_p(x_c)\beta\hbar/2)}{\sinh(\Omega_p(x_c)\beta\hbar/2)} \times \exp\left\{-\beta V_p - \frac{\beta m \Omega_p(x_c)^2}{2}(x_c - x_p)^2\right\} \tag{44}$$

If the value of $\Omega_p(x_c)$ is real, the centroid density of eq 44 represents a bound state case. An imaginary value of $\Omega_p(x_c)$ with its absolute value being smaller than $2\pi/\beta\hbar$ can represent the moderately steep unbound state where the centroid density is still defined. On the basis of the above expression and the similar expression for the reactant centroid density in eq 27, the primary factor determining the relative values of these two terms is the difference $V_r - V_p$. If this is much different than zero and positive, the product centroid density will be significantly larger than the reactant contribution for any value of the centroid constraint x_c near the location of the barrier top.

E. Analysis. One of the assumptions involved in the PI-QTST and its improved versions is that the path centroid is a natural variable that can differentiate the reactant, the barrier, and the product parts of the partition function. As we shall see, this assumption is at the heart of the problem when applying PI-QTST to strongly asymmetric or metastable potentials at low temperatures using numerical path integral methods to compute the centroid density. Indeed, in the semiclassical approximation, such an assumption is not necessary if one decomposes the centroid density into its constituent components as in the preceding sections. One can then apply the unified theory of CV using the semiclassical expressions for the centroid densities from the previous subsections. Defining the reactant partition function as

$$Z^{sc}_{c,r} = \sqrt{\frac{m}{2\pi\beta\hbar^2}} \int_{-\infty}^{x_c^*} \mathrm{d}x_c\, \rho^{sc}_{c,r}(x_c) \tag{45}$$

with $\rho^{sc}_{c,r}(x_c)$ the reactant centroid density defined in section

III.B, the rate expression is given by

$$k_{CV}^{sc} = \min\left(\frac{\omega_b}{\omega_{c,b}}, \frac{2\pi}{\omega_{c,b}\beta\hbar}\right)\frac{1}{2\pi\beta\hbar}\frac{\rho_{c,b}^{sc}(x_c^*)}{Z_{c,r}^{sc}} \quad (46)$$

where $\rho_{c,b}^{sc}(x_c^*)$ is the value of the barrier centroid density defined in section III.C evaluated at its minimum value.

At high temperatures, the barrier centroid density can be expressed as eq 37 or its variational version with ω_b replaced with $\Omega_b(x_c)$. Therefore,

$$k_{CV}^{sc} = \frac{1}{2\pi\beta\hbar}\frac{(\omega_b\beta\hbar/2)}{\sin(\Omega_b(x_c^*)\beta\hbar/2)}\frac{e^{-\beta V_b}}{Z^{sc}_{c,r}}, \quad \beta\hbar < 2\pi/\omega_b \quad (47)$$

where $\Omega_b(x_c^*)$ is the frequency of the effective inverted harmonic function fitting the maximum of the effective barrier centroid potential $V_c(x_c)$ and is seen to be equal to $\omega_{c,b}$, defined in section II. In the low temperature limit where there appears a periodic orbit, the barrier centroid density of eq 42 can be used. The resulting expression is

$$k_{CV}^{sc} = \frac{1}{\sqrt{2\pi\hbar}}\left|\frac{dE}{d(\beta\hbar)}\right|^{1/2}\frac{e^{-S_{po}/\hbar}}{Z_{c,r}^{sc}}, \quad \beta\hbar \geq 2\pi/\omega_b \quad (48)$$

This is of the same form as the Affleck's rate expression below the crossover temperature.[24,25] That is, within the semiclassical approximation, the unified theory of CV is equivalent to the bounce theory below the crossover temperature, *as long as the correct barrier part of the centroid density is used*.

In actual numerical path integral simulations, different parts of the centroid density cannot be separated and the calculated numerical value at a given centroid is the summation from all the contributions. To better understand this issue, eq 18 can be rewritten as

$$\rho_c^{sc}(x_c^*) = \rho_{c,b}^{sc}(x_c^*)\left[\frac{\rho_{c,r}^{sc}(x_c^*)}{\rho_{c,b}^{sc}(x_c^*)} + \frac{\rho_{c,p}^{sc}(x_c^*)}{\rho_{c,b}^{sc}(x_c^*)} + 1\right] \quad (49)$$

Note that this expression in this case is to be evaluated at or near the barrier ($x_c = x_c^*$). On the basis of the analysis of this section, one would clearly wish to have the term in brackets as close to unity as possible in order for any centroid-based approach such as PI-QTST or CV theory to be accurate for the rate constant. The first term inside of the bracket should always be quite small, essentially because this is what defines an activated rate process. Even in the classical limit, the intrinsic nonlinearity of the potential in the barrier region causes $\rho_{c,p}^{sc}(x_c^*)$ to be much larger than $\rho_{c,r}^{sc}(x_c^*)$ which, according to eq 27, effectively corresponds to the density from a cusped barrier at $x = x_c^*$. By contrast, the second term in the bracket in eq 49 is larger than the first term by a factor of $e^{\beta(V_r - V_p)}$, though it will still be quite small in the classical, or nearly classical, limit. On the other hand, for strongly exothermic systems at low temperature, the second term begins to be much larger and creates the situation $\rho_c^{sc}(x_c^*) \gg \rho_{c,p}^{sc}(x_c^*)$, thus leading to the serious overestimation of the rate when PI-QTST is used with a numerically determined centroid density. A similar situation occurs if $\Omega_p(x_c^*)^2$ in eq 44 becomes effectively negative, as can be the case for metastable potentials.

The analysis presented above is only valid within the semiclassical approximation. For the more general situation where one should go beyond the semiclassical limit, the separation of the centroid density into different parts is not possible and the analysis becomes unclear. However, such a semiclassical perspective provides a framework in which to understand the simple correction method presented in section III. That is, within this simple scheme, the lower bound of V_r in eq 10 seems to be an optimal choice because it does not change the barrier contribution to the centroid density but minimizes the spurious product contribution to this quantity described in the preceding paragraph. Thus a numerically determined path integral centroid density for the modified potential becomes much closer to the barrier part of this quantity as identified semiclassically. The modification procedure therefore results in an improvement in the estimation of the reaction rate using PI-QTST or CV theory in conjunction with numerical path integral methods. This approach also allows for the computational benefits of PI-QTST to be preserved in a straightforward manner. It should be noted that all of the analysis presented until now assumed that the product state potential bottom lies lower than that of the reactant state, which corresponds to an exothermic reaction. In the opposite situation of an endothermic reaction, similar analysis and conclusion are possible by reversing the role of the reactant and the product states. This is discussed in Appendix D.

V. Concluding Remarks

The PI-QTST and its variants[29,36,37] were tested in this paper for an asymmetric Eckart barrier and compared with other recent QTSTs.[43−45,55] The results show that all the theories overestimate the reaction rate as has been reported before.[41,42] The CV theory[36] is shown to be better than the other approaches in the low temperature limit. On the other hand, the CV theory is worse than the semiclassical bounce theory.[20,24,54] This is in contrast to the case of symmetric Eckart barrier, where the CV theory gives results comparable to the bounce theory.[36] When a simple correction method is employed which modifies the potential such that the product part of the potential never lies lower than the reactant well bottom potential energy, both PI-QTST and CV theory again are seen to give results comparable to those based on the bounce theory.

The present semiclassical analysis of the centroid density has provided two important findings. First, if only the barrier part of the centroid density is used, which is possible within the semiclassical approximation, the CV theory becomes equivalent to the bounce theory in the low temperature limit. Second, the effect of the simple correction mechanism to PI-QTST and CV theory presented in section III can be understood. The correction does not change the barrier part of the centroid density, but it reduces the spurious product contribution to the centroid density which arises in numerical path integral calculations. In this regard, the choice of V_r as the cutoff value seems to be the optimal choice because it is the value that makes the contribution from the product part minimal without affecting the barrier part [cf. eq 49 and the subsequent discussion].

For multidimensional cases, the correction method and the semiclassical analysis can be generalized in a straightforward way as long as the additional nonreactive degrees of freedom are coupled linearly. If there is nonlinear coupling, the semiclassical analysis becomes more complicated. Although the correction method of section III may become less straightforward in this case, the reaction rate calculated by such a method is still expected to be much closer to the exact one. Further analysis is needed and this will be the topic of future research. From the practical perspective, the correction method of section III seems not to have any difficulty associated with multidimensional situations. However, only applications of this approach to realistic situations can shed the appropriate light on this issue.

Acknowledgment. This research was supported by the National Science Foundation (Grant CHE-9712884). The authors thank Profs. David Reichman and Jianshu Cao for valuable comments. Seogjoo Jang is a graduate student in the Department of Chemistry, University of Pennsylvania.

Appendix A

Centroid Constrained Quadratic Path Integration. In the discretized path approximation, eq 15 can be written as

$$I[x_c, \mathrm{Cl}(x)] \approx \sqrt{\frac{\hbar^2\beta}{2\pi m}} \int_{-\infty}^{\infty} \mathrm{d}\zeta \exp\{i\zeta(x_{\mathrm{cl},0} - x_c)\} \times \left(\frac{m}{2\pi\epsilon\hbar}\right)^{P/2} \int \mathrm{d}y_1 \cdots \int \mathrm{d}y_{P-1} \exp\left\{-\frac{m}{2\epsilon\hbar}\mathbf{y}^T\cdot\mathbf{D}_{P-1}\cdot\mathbf{y} + \frac{i\zeta}{P}(y_1 + \cdots + y_{P-1})\right\} \quad \text{(A1)}$$

with

$$\mathbf{y}^T = (y_1, \cdots, y_{P-1}) \quad \text{(A2)}$$

and

$$\mathbf{D}_{P-1} = \begin{pmatrix} 2 + \frac{\epsilon^2}{m}V_1'' & -1 & 0 & \cdots & 0 \\ -1 & 2 + \frac{\epsilon^2}{m}V_2'' & -1 & \cdots & 0 \\ \vdots & \vdots & & & \vdots \\ 0 & 0 & 0 & \cdots & -1 \\ 0 & 0 & 0 & \cdots & 2 + \frac{\epsilon^2}{m}V_{P-2}'' \end{pmatrix} \quad \text{(A3)}$$

There are $P - 1$ eigenvalues and eigenvectors which satisfy

$$\mathbf{D}_{P-1}\cdot\mathbf{u}^{(k)} = \lambda_k\mathbf{u}^{(k)}, \quad k = 1, \cdots, P-1 \quad \text{(A4)}$$

along with the normalization condition

$$\sum_{j=1}^{P-1} u_j^{(k)} u_j^{(l)} = \delta_{kl} \quad \text{(A5)}$$

Then, introducing the following unitary matrix,

$$\mathbf{U} = (\mathbf{u}^{(1)}, \cdots, \mathbf{u}^{(P-1)}) \quad \text{(A6)}$$

and the relevant coordinate transformation

$$\mathbf{z} = \mathbf{U}^T\mathbf{y} \quad \text{(A7)}$$

Equation A1 can be simplified to

$$I[x_c, \mathrm{Cl}(x)] \approx \sqrt{\frac{\hbar^2\beta}{2\pi m}}\left(\frac{m}{2\pi\epsilon\hbar}\right)^{P/2} \int_{-\infty}^{\infty} \mathrm{d}\zeta \exp\{i\zeta(x_{\mathrm{cl},0} - x_c)\} \int \mathrm{d}z_1 \cdots \int \mathrm{d}z_{P-1} \exp\left\{-\frac{m}{2\epsilon\hbar}(\lambda_1 z_1^2 + \cdots + \lambda_{P-1} z_{P-1}^2) + i\zeta(\alpha_1 z_1 + \cdots + \alpha_{P-1} z_{P-1})\right\} \quad \text{(A8)}$$

where

$$\alpha_k = \frac{1}{P}\sum_{j=1}^{P-1} U_{jk} = \frac{1}{P}\sum_{j=1}^{P-1} u_j^{(k)} \quad \text{(A9)}$$

In this expression, each λ_k and α_k depends on x and the classical trajectory $\mathrm{Cl}(x)$.

By completing the square with respect to each z_k in the exponent of eq A8, one can reduce the discretized path integral into independent Gaussian integrations. However, if there is a negative eigenvalue, the integration over the unstable mode diverges and the centroid constrained path integration may not be defined. In this case, in fact, the centroid constraint should be imposed before integrating over the unstable mode. With some restrictions, this makes the originally unstable mode stable and a convergent expression for the centroid density can be obtained. The case where all the eigenvalues are positive is treated in Appendix B, and the case where there is one negative eigenvalue is considered in Appendix C.

Appendix B

All Positive Eigenvalues. In this case, the integrations over each z_k in eq A8 can be made by completing the squares. The resulting expression contains an exponential of a quadratic expression in terms of ζ, which can again be integrated over, leading to

$$I[x_c, \mathrm{Cl}(x)] \approx \sqrt{\frac{\beta\hbar}{\epsilon}}\prod_{k=1}^{P-1}\lambda_k^{-1/2}\sqrt{\frac{m\beta}{2\pi\gamma_P}} \times \exp\left\{-\frac{m\beta(x_{\mathrm{cl},0} - x_c)^2}{2\gamma_P}\right\} \quad \text{(B1)}$$

where

$$\gamma_P = \frac{(\beta\hbar)^2}{P}\left(\frac{\alpha_1^2}{\lambda_1} + \cdots + \frac{\alpha_{P-1}^2}{\lambda_{P-1}}\right) \quad \text{(B2)}$$

The exact value of $I[x_c, \mathrm{Cl}(x)]$ is obtained in the limit $P \to \infty$. In this limit, according the theorem of Gel'fand and Yaglom,[18,19,60]

$$\lim_{P\to\infty} \epsilon\prod_{k=1}^{P-1}\lambda_k = f(\beta\hbar) \quad \text{(B3)}$$

where $f(\tau)$ is the homogeneous solution of the differential operator of eq 16

$$\int_0^{\beta\hbar} \mathrm{d}\tau'\, L(\tau, \tau')f(\tau') = 0 \quad \text{(B4)}$$

satisfying the boundary condition of $f(0) = 0$ and $f'(0) = 1$. On the other hand, in the same continuum limit, the quantity of eq B2 becomes the following integration of the Green function[57,58] defined by eq 17:

$$\gamma \equiv \lim_{P\to\infty}\gamma_P = \frac{1}{\beta\hbar}\int_0^{\beta\hbar}\mathrm{d}\tau\int_0^{\beta\hbar}\mathrm{d}\tau'\, G(\tau, \tau') \quad \text{(B5)}$$

which is positive for the present case. Then, the exact expression of the centroid constrained path integral of eq B1 is given by

$$I[x_c, \mathrm{Cl}(x)] = \sqrt{\frac{m\beta^2\hbar}{2\pi\gamma f(\beta\hbar)}}\exp\left\{-\frac{m\beta(x_{\mathrm{cl},0} - x_c)^2}{2\gamma}\right\} \quad \text{(B6)}$$

Appendix C:

One Negative Eigenvalue. The case where there is one negative eigenvalue and all other eigenvalues are positive is considered here. Let the negative eigenvalue be λ_1. The Gaussian

integrations over other modes with positive eigenvalues can be made first in eq A8. The resulting expression is

$$I[x_c, \mathrm{Cl}(x)] \approx \frac{1}{2\pi}\sqrt{\frac{\beta\hbar}{\epsilon}}\sqrt{\frac{m}{2\pi\epsilon\hbar}}\left(\prod_{k=2}^{P-1}\lambda_k^{-1/2}\right)\int_{-\infty}^{\infty}\mathrm{d}\zeta\int_{-\infty}^{\infty}\times \mathrm{d}z_1\exp\left\{-\frac{\gamma'_P\zeta^2}{2m\beta}+i\zeta(x_{\mathrm{cl},0}-x_c+\alpha_1 z_1)-\frac{m\lambda_1}{2\epsilon\hbar}z^2{}_1\right\} \quad (C1)$$

where

$$\gamma'_P=\frac{(\beta\hbar)^2}{P}\left(\frac{\alpha_2^2}{\lambda_2}+\cdots+\frac{\alpha_{P-1}^2}{\lambda_{P-1}}\right) \quad (C2)$$

In eq C1, the integration over ζ should be performed first, which is equivalent to imposing the centroid constraint first. The resulting expression is

$$I[x_c, \mathrm{Cl}(x)] \approx \sqrt{\frac{\beta\hbar}{\epsilon}}\sqrt{\frac{m}{2\pi\epsilon\hbar}}\left(\prod_{k=2}^{P-1}\lambda_k^{-1/2}\right)\times e^{-m\beta(x_{\mathrm{cl},0}-x_c)^2/(2\gamma_P)}\int_{-\infty}^{\infty}\mathrm{d}z_1\left(\frac{m\beta}{2\pi\gamma'_P}\right)^{1/2}\times \exp\left\{-\frac{m\lambda_1\gamma_P}{2\epsilon\hbar\gamma'_P}\left(z_1+\frac{\alpha_1(\beta\hbar)^2(x_{\mathrm{cl},0}-x_c)}{P\lambda_1\gamma_P}\right)^2\right\} \quad (C3)$$

where it has been assumed that α_1 is nonzero and $\gamma_P=\gamma'_P+(\beta\hbar)^2\alpha_1/(P\lambda_1)$ is the same quantity previously defined by eq B2. Since λ_1 is negative and γ'_P defined by eq C2 is positive, the integration over z_1 in eq C3 can be performed only when the following condition is satisfied:

$$\gamma_P < 0 \quad (C4)$$

Performing integration over z_1 in eq C3 assuming the condition of eq C4,

$$I[x_c, \mathrm{Cl}(x)] \approx \left\{\frac{\beta\hbar}{\epsilon}\left(\prod_{k=1}^{P-1}\lambda_k^{-1}\right)\frac{m\beta}{2\pi\gamma_P}\right\}^{1/2}\times \exp\left\{-\frac{m\beta(x_{\mathrm{cl},0}-x_c)^2}{2\lambda_P}\right\} \quad (C5)$$

where the quantity within the square root of the preexponential factor is positive. In the limit $P\rightarrow\infty$, as is the case of Appendix B, this becomes

$$I[x_c, \mathrm{Cl}(x)] = \sqrt{\frac{m\beta^2\hbar}{2\pi f(\beta\hbar)\gamma}}\exp\left\{-\frac{m\beta(x_{\mathrm{cl},0}-x_c)^2}{2\gamma}\right\} \quad (C6)$$

which has the same form as eq B6 with the same definitions of $f(\beta\hbar)$ and γ given by eqs B3 and B5. The difference here is that both $f(\beta\hbar)$ and γ are negative.

It is important to clarify the conditions of existence of eq C6 again. The derivation of eq C3 required that both γ'_P and α_1 are nonzero. In fact, as long as α_1 is nonzero, the integration over z_1 can be made even if γ'_P is zero, which has the same form as eq C5. Therefore, the only required conditions are that (i) $\alpha_1 \neq 0$ and that (ii) $\gamma < 0$. Note that $f(\beta\hbar)$ is negative due to the condition that there is only one negative eigenvalue and no zero eigenvalue. The condition of (i) implies that motion along the unstable mode should accompany a change in the centroid position.

The quantities of $f(\beta\hbar)$ and γ appearing in eq C6 can be expressed in terms of the underlying classical trajectory. First, $f(\beta\hbar)$ is considered. One can show that the differential operator of eq 16, along the given classical trajectory $x_{\mathrm{cl}}(\tau)$, has $\dot{x}_{\mathrm{cl}}(\tau)$ as its homogeneous solution, although this may not satisfy the given boundary condition. In terms of the linear combination of this solution and the second independent solution generated from this, one can construct the following homogeneous solution:[18,19,57−59]

$$f(\tau)=\dot{x}_{\mathrm{cl}}(0)\dot{x}_{\mathrm{cl}}(\tau)\int_0^{\tau}\frac{\mathrm{d}\tau'}{\dot{x}_{\mathrm{cl}}(\tau')^2} \quad (C7)$$

One can show that this is the solution of the differential operator of eq 16 satisfying the boundary condition[18,19,60] of $f(0)=0$ and $\dot{f}(0)=1$. Special care should be taken in performing the integration over τ' in eq C7. When $\tau=\tau_0$ with $\dot{x}_{\mathrm{cl}}(\tau_0)=0$, the quantity of eq C7 can be defined as the limiting situation. When $\tau>\tau_0$, the integration can be defined only on a contour which goes around the singularity at τ_0 by gaining a small imaginary term. Due to this nature of the integration contour, the integral in eq C7 can have a negative value. With this point being clarified,

$$f(\beta\hbar)=\dot{x}_{\mathrm{cl}}(0)\dot{x}_{\mathrm{cl}}(\beta\hbar)\int_0^{\beta\hbar}\frac{\mathrm{d}\tau'}{\dot{x}_{\mathrm{cl}}(\tau')^2}=m\dot{x}_{\mathrm{cl}}(0)\dot{x}_{\mathrm{cl}}(\beta\hbar)\frac{\partial T_{\mathrm{cl}}(E,x)}{\partial E} \quad (C8)$$

where the second equality is the special case ($k=0$) of the following general identity:

$$\int_0^{\beta\hbar}\mathrm{d}\tau\frac{x_{\mathrm{cl}}(\tau)^k}{\dot{x}_{\mathrm{cl}}(\tau)^2}=m\frac{\partial}{\partial E}\int_0^{T_{\mathrm{cl}}(E,x)}\mathrm{d}\tau x_{\mathrm{cl}}(\tau;E,x)^k \quad (C9)$$

with $T_{\mathrm{cl}}(E,x)=\beta\hbar$ and E being the negative of the classical energy for the motion on the inverted potential satisfying the following relation:

$$\frac{m}{2}\dot{x}_{\mathrm{cl}}(\tau)^2-V(x_{\mathrm{cl}}(\tau))=-E \quad (C10)$$

The verification of eq C9 can be made through a change of integration variable from τ into x and then performing a partial integration. Care should be taken in taking the limit such that the divergent quantities cancel out.

Second, the quantity of γ can be expressed in a similar way. For this purpose, the Green function defined by eq 17 should be obtained first. Through the Wronski construction,[19,57−59] one can show that

$$G(\tau,\tau')=\dot{x}_{\mathrm{cl}}(\tau)\dot{x}_{\mathrm{cl}}(\tau')\int_0^{\tau_<}\frac{\mathrm{d}\tau_1}{\dot{x}_{\mathrm{cl}}(\tau_1)^2}\int_{\tau_>}^{\beta\hbar}\frac{\mathrm{d}\tau_2}{\dot{x}_{\mathrm{cl}}(\tau_2)^2}\Big/\int_0^{\beta\hbar}\frac{\mathrm{d}\tau_3}{\dot{x}_{\mathrm{cl}}(\tau_3)^2} \quad (C11)$$

where $\tau_<=\min(\tau,\tau')$ and $\tau_>=\max(\tau,\tau')$. The integration of

this Green function given by eq C11 over τ and τ' leads to

$$\int_0^{\beta\hbar} d\tau \int_0^{\beta\hbar} d\tau' G(\tau,\tau') = \int_0^{\beta\hbar} d\tau \frac{x_{cl}(\tau)^2}{\dot{x}_{cl}(\tau)^2} - \left(\int_0^{\beta\hbar} d\tau \frac{x_{cl}(\tau)}{\dot{x}_{cl}(\tau)^2}\right)^2 \Big/ \left(\int_0^{\beta\hbar} \frac{d\tau}{\dot{x}_{cl}(\tau)^2}\right) \quad \text{(C12)}$$

Using eq C9 with $k = 1, 2$, one can show that eq C12 can be written as

$$\int_0^{\beta\hbar} d\tau \int_0^{\beta\hbar} d\tau' G(\tau,\tau') = m \frac{\partial T_{cl}(E,x)}{\partial E} \left\{ \frac{\partial}{\partial T_{cl}} \int_0^{T_{cl}} \times d\tau\, x_{cl}(\tau; T_{cl}, x)^2 - \left(\frac{\partial}{\partial T_{cl}} \int_0^{T_{cl}} d\tau\, x_{cl}(\tau; T_{cl}, x)\right)^2 \right\} \quad \text{(C13)}$$

Therefore, γ defined by eq B5 is given by

$$\gamma = \frac{m}{\beta\hbar} \frac{\partial T_{cl}(E,x)}{\partial E} \left\{ \frac{\partial}{\partial T_{cl}} \int_0^{T_{cl}} d\tau\, x_{cl}(\tau; T_{cl}, x)^2 - \left(\frac{\partial}{\partial T_{cl}} \int_0^{T_{cl}} d\tau\, x_{cl}(\tau; T_{cl}, x)\right)^2 \right\} \quad \text{(C14)}$$

Appendix D

Case of an Endothermic Reaction. In this case, a similar analysis can be made by reversing the roles of the reactant and the product states in the semiclassical analysis of section IV. Then, in the strongly endothermic case, the following situation can occur:

$$\rho^{sc}_{c,r}(x^*_c) \gg \rho^{sc}_{c,b}(x^*_c) \quad \text{(D1)}$$

so that $\rho^{sc}_{c}(x^*_c) \gg \rho^{sc}_{c,b}(x^*_c)$ according to eq 49. That is, the mixing-in of the reactant part and the barrier part of the centroid density can lower the effective barrier, which can result in the overestimation of the reaction rate when using numerical path integral methods to calculate the overall centroid density in the barrier region. This error can be corrected in the following way. For the calculation of the reactant partition function, the centroid potential of mean force for the original potential would be used. For the calculation of the centroid density in the barrier region, however, the simulation would be performed for the following modified potential:

$$V(x) = \begin{cases} V(x), & V(x) \geq V_p \\ V_p, & V(x) < V_p \end{cases} \quad \text{(D2)}$$

where V_p is the bottom value of the product part of the potential. The PI-QTST or CV theory given by eq 5 can then be applied using the reactant partition function calculated from the original potential with the centroid potential of mean force for the barrier contribution to the formula calculated with the modified potential of eq D2. This procedure will result in a reaction rate which satisfies detailed balance and becomes comparable to the semiclassical results in the low temperature limit.

References and Notes

(1) Pechukas, P. In *Dynamics of Molecular Collisions, Part B*; Miller, W. H., Ed.; Plenum: New York, 1976.
(2) Truhlar, D. G.; Hase, W. L.; Hynes, J. T. *J. Phys. Chem.* **1983**, *2664*, 87.
(3) Hynes, J. T. In *Theory of Chemical Reaction Dynamics*; Baer, M., Ed.; CRC Press: Boca Raton, 1985.
(4) Chandler, D. *J. Stat. Phys.* **1986**, *49*, 42.
(5) Onuchic, J. N.; Wolynes, P. G. *J. Phys. Chem.* **1988**, *6495*, 92.
(6) Hänggi, P.; Talkner, P.; Borkovec, M. *Rev. Mod. Phys.* **1990**, *251*, 62.
(7) Voth, G. A. *J. Phys. Chem.* **1993**, *8365*, 97.
(8) Anderson, J. B. *Adv. Chem. Phys.* **1995**, *381*, 91.
(9) Pollak, E. In *Dynamics of Molecules and Chemical Reactions*; Wyatt, R. E., Zhang, J. Z. H. Marcel Dekker: New York, 1996.
(10) Refer to refs 1−9 and the references cited therein.
(11) Yamamoto, T. *J. Chem. Phys.* **1960**, *281*, 33.
(12) Miller, W. H. In *Dynamics of Molecules and Chemical Reactions*; Wyatt, R. E., Zhang, J. Z. H., Eds.; Marcel Dekker: New York, 1996.
(13) Miller, W. H. *J. Phys. Chem. A* **1998**, *793*, 102.
(14) Wigner, E. P. *Z. Phys. Chem. Abt. B* **1932**, *203*, 19.
(15) Wolynes, P. G. *Phys. Rev. Lett.* **1981**, *968*, 47.
(16) Feynman, R. P.; Hibbs, A. R. *Quantum Mechanics and Path Integrals*; McGraw-Hill Book Company: New York, 1965.
(17) Feynman, R. P. *Statistical Mechanics*, Addison-Wesley Publishing Company: New York, 1972.
(18) Schulman, L. S. *Techniques and Applications of Path Integration*; Wiley-Interscience: New York, 1981.
(19) Kleinert, H. *Path Integrals in Quantum Mechanics, Statistics, and Polymer Physics*; World Scientific: Singapore, 1995.
(20) Miller, W. H. *J. Chem. Phys.* **1975**, *1899*, 62.
(21) Callan, J. C. G.; Coleman, S. *Phys. Rev. D* **1977**, *1762*, 16.
(22) Coleman, S. *Phys. Rev. D* **1977**, *2929*, 15.
(23) Coleman, S. In *The Why's of Subnuclear Physics*; Zichichi, A., Ed.; Plenum: New York, 1979.
(24) Affleck, I. *Phys. Rev. Lett.* **1981**, *388*, 46.
(25) Hänggi, P.; Hontscha, W. *J. Chem. Phys.* **1988**, *4094*, 88.
(26) Benderskii, V. A.; Goldanskii, V. I.; Makarov, D. E. *Phys. Rep.* **1993**, *195*, 233.
(27) Nakamura, T.; Ottewill, A.; Takagi, S. *Ann. Phys.* **1997**, *9*, 87.
(28) Gillan, M. J. *J. Phys. C* **1987**, *3621*, 20.
(29) Voth, G. A.; Chandler, D.; Miller, W. H. *J. Chem. Phys.* **1989**, *7749*, 91.
(30) McRae, R. P.; Schenter, G. K.; Garrett, B. C.; Haynes, G. R.; Voth, G. A.; Schatz, G. C. *J. Chem. Phys.* **1992**, *7392*, 97.
(31) Toapler, M.; Makri, N. *J. Chem. Phys.* **1994**, *7500*, 101.
(32) Voth, G. A. *Adv. Chem. Phys.* **1996**, *135*, 93.
(33) Stuchebrukhov, A. A. *J. Chem. Phys.* **1991**, *4258*, 95.
(34) Messina, M.; Schenter, G. K.; Garrett, B. C. *J. Chem. Phys.* **1993**, *8525*, 98.
(35) Messina, M.; Schenter, G. K.; Garrett, B. C. *J. Chem. Phys.* **1993**, *8644*, 99.
(36) Cao, J.; Voth, G. A. *J. Chem. Phys.* **1996**, *6856*, 105.
(37) Ramirez, R. *J. Chem. Phys.* **1997**, *3550*, 107.
(38) Cao, J.; Voth, G. A. *J. Chem. Phys.* **1997**, *1769*, 106.
(39) Schwieters, C. D.; Voth, G. A. *J. Chem. Phys.* **1998**, *1055*, 108.
(40) Schwieters, C. D.; Voth, G. A. *J. Chem. Phys.* **1999**. In press.
(41) Makarov, D. E.; Topaler, M. *Phys. Rev. E* **1995**, *178*, 52.
(42) Mills, G.; Schenter, G. K.; Makarov, D. E.; Jónsson, H. *Chem. Phys. Lett.* **1998**, *91*, 278.
(43) Hansen, N. F.; Andersen, H. C. *J. Chem. Phys.* **1994**, *6032*, 101.
(44) Hansen, N. F.; Andersen, H. C. *J. Phys. Chem.* **1996**, *1137*, 100.
(45) Pollak, E.; Liao, J.-L. *J. Chem. Phys.* **1998**, *2733*, 108.
(46) Miller, W. H.; Schwartz, S. D.; Tromp, J. W. *J. Chem. Phys.* **1993**, *4889*, 79.
(47) Giachetti, R.; Tognetti, V. *Phys. Rev. Lett.* **1985**, *912*, 55.
(48) Feynman, R. P.; Kleinert, H. *Phys. Rev. A* **1986**, *5080*, 34.
(49) Parrinello, M.; Rahman, A. *J. Chem. Phys.* **1984**, *861*, 80.
(50) Cao, J.; Berne, B. J. *J. Chem. Phys.* **1989**, *6359*, 91.
(51) Tuckerman, M. E.; Berne, B. J.; Martyna, G. J.; Klein, M. L. *J. Chem. Phys.* **1993**, *2796*, 99.
(52) Martyna, G. J.; Klein, M. L.; Tuckerman, M. *J. Chem. Phys.* **1992**, *2635*, 97.
(53) Jang, S.; Voth, G. A. *J. Chem. Phys.* **1997**, *9514*, 107.
(54) Hanggi, P.; Hontscha, W. *Ber. Bunsen-Ges. Phys. Chem.* **1991**, *379*, 95.
(55) Shao, J.; Liao, J.; Pollak, E. *J. Chem. Phys.* **1998**, *9711*, 108.
(56) Hontscha, W.; Hanggi, P.; Riseborough, P. *Phys. Rev. B* **1990**, *2210*, 41.
(57) Courant, R.; Hilbert, D. *Methods of Mathematical Physics*; Interscience Publishers, Inc.: New York, 1953; Vol. 1.
(58) Mathews, J.; Walker, R. L. *Mathematical Methods of Physics*; W. A. Benjamin, Inc.: Menlo Park, California, 1969.
(59) Dashen, R.; Hasslacher, B.; Neveu, A. *Phys. Rev. D* **1974**, *4114*, 10.
(60) Gel'fand, I. M.; Yaglom, A. M. *J. Math. Phys.* **1960**, *48*, 1.